**Biogeosciences
Discussions**

Sensitivity of North Patagonian temperate rainforests to changes in rainfall regimes: a process-based, dynamic forest model

A. G. Gutiérrez[1,*], J. J. Armesto[2,3], M. F. Díaz[4], and A. Huth[1]

[1]Department of Ecological Modeling, Helmholtz Centre for Environmental Research (UFZ), Leipzig, Germany
[2]Instituto de Ecología y Biodiversidad (IEB), Facultad de Ciencias, Universidad de Chile, Santiago, Chile
[3]Center for Advanced Studies in Ecology & Biodiversity (CASEB), Santiago, Chile
[4]Departamento de Ciencias Biológicas, Facultad de Ciencias Biológicas, Universidad Andrés Bello, Santiago, Chile
[*]now at: Forest Ecology, Institute of Terrestrial Ecosystems, Department of Environmental Sciences, Swiss Federal Institute of Technology ETH, Universitätstr. 22, 8092 Zürich, Switzerland

Correspondence to: A.G. Gutiérrez (alvaro.gutierrez@env.ethz.ch)

Abstract

Rainfall changes due to climate change and their potential impacts on forests demand the development of predictable tools coupling vegetation dynamics to hydrologic processes. Such tools need to be accurate at local scales (i.e. < 100 ha) to develop efficient forest management strategies for climate change adaptation. In this study, we developed and tested a dynamic forest model to predict hydrological balance of North Patagonian temperate rainforests on Chiloé Island, Chile (42° S). The developed model includes detailed calculations of forest water fluxes and incorporates the dynamical linkage of rainfall regimes to soil moisture, and individual tree growth. We confronted model results with detailed field measurements of water fluxes in a young secondary stand (YS). We used the model to compare forest sensitivity in the YS and an old-growth stand (OG, > 500 yr-old), i.e. changes in forest evapotranspiration, soil moisture and forest structure (biomass and basal area). We evaluated sensitivity using changes in rainfall regimes comparable to future climatic scenarios for this century in the study region. The model depicted well the hydrological balance of temperate rainforests. We found a higher evapotranspiration in OG than YS under current climatic conditions. Dryer climatic conditions predicted for this century in the study area led to changes in the hydrological balance that impacted forest structure, with stronger impacts in OG. Changes in climatic parameters decreased evapotranspiration (up to 15 % in OG compared to current values) and soil moisture to 32 % . These changes in water fluxes induced decreases in above-ground biomass in OG (up to 27 %). Our results support the use of the model for detailed analyses of climate change impacts on hydrological balance of forests. Also, it provides a tool suitable for analyses of the impacts of multiple drivers of global change on forest processes (e.g., climate change, fragmentation, forest management).

1   Introduction

Climate and forests are dynamically linked through the spatial and temporal variability of soil moisture (Rodriguez-Iturbe et al., 1999), with feedbacks operating between climatic and ecological processes that need to be understood. Forest dynamics models,
5 particularly those based on interactions among individual trees (i.e. gap models Botkin et al., 1973; Shugart, 1984; Bugmann, 2001), provide a simple and general modeling framework to address these dynamic feedbacks. Gap models simulate the fate of single trees on the basis of species' life-history traits and limited resource availability (e.g., soil moisture, Botkin et al., 1973; Shugart, 1984; Bugmann, 2001), thereby facilitating
10 detailed analyses of climate-forest interactions.

   A key challenge in the development of forest gap models is the dynamic coupling of ecological and hydrological processes to predict the response of forests to climate change (Reynolds et al., 2001; Asbjornsen et al., 2011; Vose et al., 2011). Forest gap models use simplified assumptions of soil moisture dynamics and forest water
15 fluxes to predict forest dynamics (Bugmann and Cramer, 1998; Bugmann, 2001). Although these models have produced accurate predictions of forest composition over large spatial scales (Bugmann and Solomon, 2000), they lack detail at local scales (i.e. < 100 ha) to simulate forest hydrological components such as evapotranspiration. Local alterations of rainfall regimes influence soil moisture dynamics, hampering productivity
20 due to changes in the duration and frequency of periods of water stress (Porporato et al., 2004). This water stress-induced changes in forest productivity at local scales are relevant for developing consistent forest management strategies to adapt forests to climate change (Vose et al., 2011), particularly in fragmented forest landscapes (Díaz et al., 2007).
25 Forest gap models have successfully simulated dynamics in a variety of forest types including temperate rainforests of the Southern Hemisphere (Hall and Hollinger, 2000; Gutiérrez and Huth, 2012). In southern South America (SSA, 37–43° S), the progressive loss, fragmentation and subsequent degradation of temperate rainforests due to

A. G. Gutiérrez et al.

unsustainable logging and fire is occurring at unprecedented fast rates threatening the integrity of ecosystem functions (Echeverría et al., 2007; Rüger et al., 2007; Lara et al., 2009) and modifying hydrological balance of forests (Díaz et al., 2007; Little et al., 2009). In addition, annual precipitation has decreased in the same region by 40 % in the last century (time period 1901–2005, Trenberth et al., 2007) and can decrease up to 50 % for year 2100 with changes being largest in summer (DGF and CONAMA, 2006; Christensen et al., 2007). Forests in SSA share similar structural characteristics to temperate rainforests found in the Pacific Northwest of North America, South-Eastern Australia, and New Zealand (Alaback, 1991) and represent the largest area of temperate forests remaining in the Southern Hemisphere (Armesto et al., 2009). Floristic richness of these forests is the highest among temperate rainforests worldwide and the high concentration of endemism has given this region a unique global conservation value (Armesto, 1998; Armesto et al., 2009). The global relevance of these forests and climatic trends predicted for this century demand to expand model applications into this region to predict temperate rainforests sensitivity to climate change.

In this study, we developed a forest gap model to analyze the sensitivity of temperate rainforests of Southern Chile to changes in rainfall regimes. The developed model provides detailed calculations of forest water fluxes and incorporates a dynamical linkage of rainfall regimes, soil moisture, and individual tree growth. We confronted model results with detailed field measurements of water cycling in a stand located in northern Chiloé Island, Chile (41°50′ S). After evaluating model performance, we focused on the sensitivity of model to predict changes in forest hydrology (evapotranspiration and soil moisture) and forest structure (above-ground biomass and basal area) due to rainfall regime changes comparable to those predicted by climate change scenarios in the study area. We finally compared model predictions in a young-secondary and old-growth stand to analyze differences in forest sensitivity to changes in rainfall regimes.

2 Material and methods

2.1 Study area

The study was conducted at *Estación Biológica Senda Darwin*, northern Chiloé Island, Chile (EBSD, 41°50′ S, Fig. 1). Fragments of secondary and primary forests occur over rolling hills of low altitude (50–100 m) dispersed in a matrix of bogs, shrublands and artificial grasslands. The present landscape has been shaped by a history of widespread use of fire to clear land for pastures since late 1800s followed by selective logging of remaining forest patches (Willson and Armesto, 1996). Soils are generally thin (< 0.5 m), originated from Pleistocenic moraine fields and glacial outwash plains, often with poor drainage (Holdgate, 1961). Soils have high organic matter content, soil texture loam to silty loam, and a 2–4 mm thick iron silicate layer or hardpan (found at ca. 52 cm depth), where roots cannot penetrate (Janssen et al., 2004; Díaz and Armesto, 2007). The prevailing climate is wet-temperate with strong oceanic influence (di Castri and Hajek, 1976). Rainfall occurs throughout the year, with an annual average of 2158 mm and a mean annual temperature of 9.1 °C. Mean maximum and minimum monthly temperatures are 13.9 °C (January) and 4.2 °C (July) (Gutiérrez et al., 2009).

Floristically, the studied forest type is defined as North Patagonian temperate rainforest (Veblen et al., 1983). The canopy is dominated by *Podocarpus nubigena* (Podocarpaceae), *Drimys winteri* (Winteraceae) and *Nothofagus nitida* (Nothofagaceae), with the common presence of *Tepualia stipularis* (Myrtaceae) and several Myrtaceae tree species in the understory. Ferns (e.g., *Hymenophyllum* spp., *Hymenoglosum cruentum, Polypodium feullei*) and angiosperms (e.g., Gesneriaceae and Bromeliaceae) growing epiphytically are frequent. A detailed description of forest structure and dynamics of this forest type can be found in Gutiérrez et al. (2004, 2009).

2.2 The forest model

Here, we present an individual-oriented dynamic forest model (FORMIND-CLIM v.1.0) that includes calculations of hydrologic balance. The model is based on FORMIND, a forest model comprehensively tested to simulate dynamics of temperate rainforests in SSA (Rüger et al., 2007; Gutiérrez and Huth, 2012). FORMIND is a generalized forest growth model that simulates the spatial and temporal dynamics of uneven-aged mixed species forest stands. The model simulates forest dynamics (in annual time steps, t) as a mosaic of interacting forest patches of 20 m × 20 m, which is the approximate crown size of a large mature tree. Within these patches, forest dynamics is driven by tree competition for light and space following the gap model approach (Shugart, 1984; Botkin, 1993). For the explicit modeling of the competition for light, each patch is divided vertically into small height layers (i.e. 0.5 m), where leaf area is summed up and the light environment in the forest interior is calculated via a light extinction law. The carbon balance of each individual tree is modeled explicitly, including the main physiological processes (photosynthesis, respiration). Growth process equations are modified from the models FORMIX3 and FORMIX3-Q (Huth and Ditzer, 2000, 2001). Allometric functions and geometrical relations are used to calculate above-ground biomass, tree height, crown diameter and stem volume from the *dbh* of the tree (dbh, stem diameter at 1.3 m height). Tree mortality can occur either through self-thinning in densely populated stands, tree senescence, gap formation by large falling trees, slow tree grow, or external disturbances (e.g., wind throws). Gap formation links neighboring forest areas. Tree regeneration rates are formulated as maximum rates of recruitment of small trees at *dbh* threshold of 1 cm, with seed loss through predation and seedling mortality being incorporated implicitly (Rüger et al., 2007). These maximum rates are reduced by shading. Nutrient availability is considered to be homogeneous at the stand scale. A detailed description of FORMIND core model and its equations can be found in Köhler (2000), Ruger et al. (2007) and Gutiérrez and Huth (2012). We focus below on the extensions added to calculate the forest hydrological cycle.

2.3 The hydrologic model

The soil moisture dynamics is described at a daily timescale, treating the soil as a reservoir with an effective storage capacity that is intermittently filled by rainfall events. Soil water losses occur via transpiration, interception by the forest canopy, and drainage below the root zone. We neglected lateral water flow, thus the model applies mainly to terrains without marked topographic effects. The soil saturation s (volume/volume, i.e. dimensionless, $0 \leq s \leq 1$), vertically averaged over the soil depth z (cm), was considered as central state variable (Porporato et al., 2004). Thus, the soil moisture balance equation at a point can be expressed as (Rodriguez-Iturbe et al., 1999):

$$n \cdot z \cdot \frac{\mathrm{d}s}{\mathrm{d}d} = I_\mathrm{d} - T_\mathrm{d} - Q(s, d) \tag{1}$$

where d is the Julian day of the year, n is the porosity (volume of voids/total volume of soil, i.e. dimensionless, vertically averaged); I_d is the net precipitation to the soil surface (mm day^{-1}); T_d is the transpiration rate (mm day^{-1}); and $Q(s, d)$ is the drainage (mm day^{-1}). Both n and z are assumed to be time-invariant parameters (Rodriguez-Iturbe et al., 1999). The volumetric water content (θ, m^3 water/m^3 soil, i.e. dimensionless) can be calculated as follows (Rodriguez-Iturbe et al., 1999):

$$\theta = \frac{s}{n} \tag{2}$$

The normalized version of Eq. (1) is used through the text where all terms are divided by $n \cdot z$. Both the local vertical and horizontal spatial variability of soil moisture are considered negligible at the daily timescale, assuming an equal propagation of the wetting front and equal soil moisture redistribution over the rooting zone (Kumagai et al., 2004; Porporato et al., 2004).

2.3.1 Net precipitation

Daily net precipitation to the soil surface (I_d) is described by,

$$I_d = P_d - Ec_d \qquad (3)$$

where, Ec_d is the canopy interception (mm day^{-1}), defined here as the total amount of daily rainfall (P_d, mm day^{-1}) that is retained by the canopy and is evaporated so that it does not reach the ground. Following Rutter and Morton (1977), we assumed that Ec_d asymptotically approaches the canopy retention capacity and can be modeled at the daily time scale as:

$$Ec_d = S_t \cdot (1 - e^{-\alpha \cdot P_d}) \qquad (4)$$

where S_t is the canopy water retention capacity of the stand at year t and α is a parameter describing the slope of the saturation curve. The parameter α represents, in a simplified way, the complex process of the partitioning of water into throughfall and stem flow (Wattenbach et al., 2005). S_t depends on canopy density and is calculated by the expression (Rey, 1999):

$$S_t = \frac{\text{LAI}_t}{\text{LAI}_{max}} \cdot Sc_t \qquad (5)$$

where LAI_t is the leaf area index of the forest at simulated year t, LAI_{max} is the maximum leaf area index of the forest and Sc_t represents the maximum storage capacity. We assumed a logarithmic relation between Sc_t and LAI_t (Wattenbach et al., 2005):

$$Sc_t = f \cdot \log(1 + \text{LAI}_t) \qquad (6)$$

where f describes the relationship between increasing leaf area index and the storage capacity (Fig. 2).

Forest sensitivity to changes in rainfall regimes

A. G. Gutiérrez et al.

2.3.2 Soil moisture modeling

Given the large rainfall intensity in the study area, it is reasonable to assume that net precipitation to the soil surface can exceed the soil infiltration capacity and leave the system through runoff. Runoff occurs when the soil is saturated and no more water can be held by the soil (i.e. $s = 1$). The excess of water is assumed to leave the system. Drainage out of the root zone ($Q(s,d)$) was modeled according to Rodriguez-Iturbe (1999). When the soil is saturated ($s = 1$), soil water is permitted to percolate at rate equivalent to the soil hydraulic conductivity of the given soil at field capacity (k_{soil}, mm day^{-1}). When $s < 1$, soil depth percolation rate is calculated using the empirical relationship of Neilson (1995), which has been broadly applied in vegetation modeling (Smith et al., 2001; Sitch et al., 2003),

$$Q(s,d) = k_{soil} s^2 \tag{7}$$

2.3.3 Transpiration

Water-use efficiency describes the proportion of water used for the assimilation of a unit of carbon in the photosynthesis (Bazzaz, 1979; Lambers et al., 1998). This concept can be used to estimate transpiration of the forest (T_d, mmol H$_2$O m^{-2} s^{-1}) from:

$$T_d = \frac{A_d}{\text{WUE}} \tag{8}$$

where, A_d is the canopy photosynthetic rate (μmol carbon dioxide m^{-2} s^{-1}) of the forest at day d and WUE is a parameter denoting the water use efficiency of the forest. Only a certain amount of water can be held and transported away from the canopy under given climatic conditions. This physical limit is described by the daily potential evapotranspiration (PET$_d$, mm day^{-1}). Evaporation is neglected in the model, therefore, it is assumed that maximum water losses by vegetation is limited by the difference between PET$_d$ and the canopy interception of the day (Ec_d), as follows:

$$\text{PET}_d - Ec_d \geq T_d \tag{9}$$

PET_d is calculated using a modified Penman-Monteith expression following standard calculations (Gerten et al., 2004; Venevsky and Maksyutov, 2007) and determined by the variation of the daily net radiation flux (Rn_d, Wm^{-2}):

$$PET_d = \left(\frac{\Delta}{\Delta + \gamma}\right) Rn_d / L \tag{10}$$

where γ is the psychometric constant (ca. $65\,PaK^{-1}$, slightly depends on temperature), L is the latent heat of vaporization of water (ca. $2.56 \times 10^6\,Jkg^{-1}$ slightly depends on temperature) and Δ is the rate of change of saturated vapor pressure with temperature (PaK^{-1}) (Prentice et al., 1993; Haxeltine and Prentice, 1996). Rn_d was calculated from latitude, day of the year, sunshine hours and daily air temperature ($Temp_d$, $^\circ C$) following Prentice et al. (1993) and Venevsky and Maksyutov (2007). The rate of increase of saturated vapor pressure was calculated by,

$$\Delta = \frac{2.503 \times 10^6 e \left(17.269 \frac{Temp_d}{237.3 + Temp_d}\right)}{(237.3 + Temp_d)^2} \tag{11}$$

2.3.4 Soil moisture impact on tree biomass production

The dependence of water uptake for tree biomass production on soil water content s is described by a function representing a reduction factor due to water scarcity ($\omega(s)$, $0 \leq \omega(s) \leq 1$, see also Dingman, 2002). This factor accounts indirectly for the impact of water demand on potential photosynthetic production and it is implemented as a daily reduction factor due to water scarcity by,

$$\omega(s) = \begin{cases} 0, & s \leq \theta_{wp} \\ (s - \theta_{wp})/(\theta_{msw} - \theta_{wp}), & \theta_{wp} < s \leq \theta_{msw} \\ 1, & s > \theta_{msw} \end{cases} \tag{12}$$

where, θ_{fc} is the soil field capacity, θ_{wp} is the wilting point, and θ_{msw} represents a threshold when enough soil moisture is available for the potential biomass production of plants (all in percentage of soil water volume). We calculated θ_{msw} from:

$$\theta_{msw} = \theta_{wp} + \frac{1}{3}(\theta_{fc} - \theta_{wp}) \tag{13}$$

In the model, the wilting point (θ_{wp}) determines the lowest soil moisture content needed for biomass production of plants. Thus, we assumed a linear reduction of biomass production when soil water content was between θ_{msw} and θ_{wp}. The required water for biomass production of trees is completely removed from the soil water content when soil moisture reach θ_{msw} (i.e., $\varpi(s) = 1$), both before the calculation of potential transpiration and after maximum possible transpiration of trees. Both biomass production and the water supply are reduced until soil moisture, after reduction of the water needed for biomass production, correspond with θ_{wp}. Transpiration is reduced until soil moisture reach exactly the critical value θ_{wp} and set to zero when soil water content is under θ_{wp} because plants can only take soil water when soil moisture is higher than the wilting point (θ_{wp}).

2.3.5 Weather generator

Rainfall time series, representing the frequency and amount of rainfall events, were constructed as series of random numbers generated by probability distributions. Following the approach of Laio et al. (2001), the interval between precipitation events, τ (day) can be expressed as an exponential distribution given by

$$f_T(\tau) = \lambda \cdot e^{-\lambda \tau}, \quad \text{for} \quad \tau \geq 0 \tag{14}$$

where $1/\lambda$ is the mean interval time between rainfall events (day). The amount of rainfall when rainfall occurs, h (mm day^{-1}), is also assumed as an independent random

variable, expressed by an exponential probability density function (Laio et al., 2001):

$$f_H(h) = \frac{1}{\eta} \cdot e^{-\frac{1}{\eta}h}, \quad \text{for} \quad h \geq 0 \tag{15}$$

where η is the mean amount of daily rainfall (mm day^{-1}). According to meteorological records from EBSD, daily global radiation (Rg_d) varied among seasons in relation to daily rainfall (T-test, $p < 0.001$). Therefore, Rg_d was related to daily rainfall (P_d) via Gaussian random variable with parameters (mean, μ, and standard deviation, σ) that vary according to P_d ($P_d < 1$ mm and $P_d \geq 1$ mm) and the season of the year. Daily temperature (°C) was simulated via a Gaussian random variable with parameters (mean, μ, and standard deviation, σ) that vary according to season of the year.

2.4   Field data

2.4.1   Stand structure

In 2007, we set up two plots of 20×20 m to measure the hydrologic balance of a young secondary forest stand (hereafter YS) in a flat area at EBSD. The YS stand was initiated from a stand-replacing fire 60 yrs ago and currently presented no evidence of logging. All trees rooted within each plot with stems > 1.3 m height and > 5 cm dbh were permanently marked with numbered aluminum tags, identified to species, and their dbh measured to the nearest cm. We characterized stand structure in terms of tree species dominance (basal area) and size (dbh) distribution.

2.4.2   Hydrologic measurements

At the two plots described above, we estimated net precipitation using measurements of throughfall (i.e. rainfall that falls through canopy gaps and leaf drip), and stemflow. We conducted these estimations during several rainfall events ($N = 14$) occurring between June 2007 to March 2009. During the same time period, we analyzed hourly

records of rainfall from the meteorological station at EBSD to obtain daily incident rainfall above the canopy. Rainfall events considered in the analysis occurred at least with a separation time of two hours without rainfall to allow the full drip from forest canopy. Stemflow collectors consisted of a 2 mm thick smooth polycarbonate sheet that was

5 molded around the stem to form a funnel. A hose led from the lowest point of the funnel to a 25 l polythene container, where the stemflow water was periodically collected after each rainfall event. We located stemflow collectors in 10 randomly selected trees of the main canopy tree species *Drimys winteri* and *Nothofagus nitida* (*dbh* > 10 cm, 10 per plot). We eliminated two trees because they died during the study period. We

10 transformed the amount of collected water to millimeters of rainfall assuming that the surface of the collectors equals the projected tree crown area. Crown area was approximated by the area of an ellipse. Throughfall collectors 0.12 × 2 m (total area of 0.7 m^2 per plot) long gutters were held, with a slight inclination, 0.5 m above the ground in three different areas of each plot. Collectors were connected with a funnel to a 25 l

15 polythene container. Soil matric potential was measured with four sensors per plot (*WatchDog Data Loggers* 450 and 800). We located sensors approximately in every quarter of each plot and beneath the canopy. Continuous soil moisture measurements were obtained every 30 min for the period January 2007 to January 2008.

2.5 Model parameterization

20 We used a previous model parameterization for North Patagonian forests including all main canopy tree species (9 genera representing 11 tree species) occurring in the studied forests. The calibration, validation and robustness of this parameter set to reproduce forest stand structure is discussed in detail by Gutiérrez and Huth (2012). Here, we detail calibration of parameters related to the inclusion of hydrologic balance

25 into the model. New parameters needed to run this model version (FORMIND-CLIM v.1.0) and their values are detailed in Table 1.

The parameter describing the relationship between leaf area index and canopy storage capacity was calibrated assuming that storage capacity reaches 4.9 mm day^{-1} at a

leaf area index 5.0 as measured by Díaz et al. (2007, Fig. 2b). LAI_{max} was set to 5.5 following the maximum value observed in Chilean temperate rainforests (Lusk, 2001). The slope of the saturation curve of the canopy rain retention capacity (α) was set according to common values of broad-leaved temperate trees (Wattenbach et al., 2005). To our knowledge no estimation exists for the water-use efficiency at stand scale in the study area. Therefore we calibrated WUE using transpiration estimates of Díaz et al. (2007) in Chiloé Island and the potential canopy photosynthetic rate estimated by the model at the study area under current climatic conditions (296 mm yr^{-1} and 32.9 t C ha^{-1}, respectively). The selected WUE (Table 1) was then confirmed with reported values in temperate rainforests elsewhere (Brodribb and Hill, 1998; Cunningham, 2005; Zuñiga et al., 2006; Piper et al., 2007). Soil characteristics (porosity and depth) followed field descriptions from Chiloé Island (Janssen et al., 2004). We set water-retention and percolation properties of the soil (parameters θ_{wp}, θ_{fc} and k_{soil}) to average parameter values (Maidment, 1993; Sitch et al., 2003). For these estimates we used soil texture classes (loam to silty loam) described by Janssen et al. (2004) in the study area. We used climatic daily records of rainfall from the meteorological station at EBSD (60 m a.s.l., period from May 1998 to February 2009) to derive climatic parameters for current climatic simulations (Table 2). Results of the weather generator were tested elsewhere (see Gutiérrez, 2010). Calibrated climatic parameters were assumed representative for the spatial scale of the study area, i.e. northern Chiloé Island.

2.6 Analyses

2.6.1 Model verification

We compared daily field data of soil moisture with model results using rainfall data for the same period that field measurements were conducted, i.e. 2008. Also, we checked the agreement of model results with field measurements of hydrologic balance in other temperate rainforests elsewhere in Chile.

We tested model performance to reproduce forest structural data by comparing simulated results against field data from YS and an old-growth forest located in the study area (hereafter OG). Structure and composition of YS is comparable to that described for young-secondary stands elsewhere on northern Chiloé Island (Table 3). Note that YS was the same stand where hydrologic measurements were taken. OG was an unmanaged forest stand > 590 yr-old, with no evidence of recent human disturbance, and representative of old-growth North Patagonian stands on Chiloé Island (Gutiérrez et al., 2009). Forest dynamics, stand history, species composition and structure of OG is described in detail in Gutiérrez et al. (2004). To assess the performance of the model to reproduce field data, we contrasted tree species basal area and stand *dbh* distributions predicted by the model with measured stand structure and *dbh* distributions of stands. The comparison for YS was done after 60 yr of succession, with succession initialized from a treeless state. For comparing OG structure, we initialized simulations with stand inventory data and run the model for 1000 yr to allow the simulated stand to reach dynamic equilibrium. We compared simulated data at the end of the simulations with OG observed structure according to Gutiérrez et al. (2004). We ran 100 simulations of 1 ha (i.e. 25 × 0.04 forest patches, 2500 patches in total) using current climatic parameters (Table 2), parameters listed in Table 1. Demographic and species parameters were taken from Gutiérrez and Huth (2012, site Tepual).

2.6.2 Sensitivity of climatic parameters

We ran simulations to test the sensitivity of model predictions to changes in forest structure and hydrological components as a response to changes in interval time and the mean amount of rainfall events parameters (parameters $1/\lambda$ and η, respectively). First, we systematically reduced η until reached 50 % of the value under current climatic conditions. Then, we increased the parameter $1/\lambda$ until reached 150 % of the value under current climatic conditions. Rainfall parameters were first varied separately (without changing the other parameter) and then together. This parameter variation produced a total of 36 climatic scenarios, including the current climatic scenario (Table 2). All

other parameters of the model were kept constant. We used as response variables the simulated total basal area and above-ground biomass. For changes in hydrological components, we focused our analysis in evapotranspiration, computed as the sum of transpiration and interception, and soil moisture because they are dynamically linked to forest processes such as individual tree growth (cf. Eq. 8). We ran simulations for both forest stands (YS and OG) to describe changes in forests at different successional stages. Simulations were initialized and ran under the same conditions described above (see Sect. 2.6.1). We ran 20 simulations per each scenario and stand (1440 simulations in total). Results were compared using the difference between mean of the studied variable under current climatic conditions and the mean of the studied variable under the climatic scenarios. All statistical analyses and figures were done using R (R-Development-Core-Team, 2005).

3   Results

3.1   Model verification

Model performance to reproduce species-level basal area of YS and OG is shown in Fig. 3a. Size distribution predicted by the model was qualitatively similar to field data (Fig. 3b), but with some departures in small dbh-classes (< 35 cm) in YS (Fig. 3b). Net precipitation predicted by the model (throughfall plus stemflow) was significantly correlated with measured values for several rainfall events (Fig. 4, $N = 14$, $p < 0.01$), with canopy interception predicted by the model during measured rainfall events in the range of field estimates (data not shown). As expected, the model predicted an increased soil moisture after finishing the growing season (Fig. 5a, $59 <$ julian day < 242) mainly triggered by a higher frequency of rainfall events and by decreased transpiration of trees. In contrast during the growing season, predicted soil moisture gradually decreased (Fig. 5a). This predicted pattern of soil moisture closely followed the measured pattern

of soil matric potential during the same time period (Fig. 5b, significantly correlated $r^2 = -0.65$, $p < 0.001$).

Model predictions for the major components of forest water balance were comparable to reported values in broad-leaved temperate rainforests in Chile and elsewhere (Table 4, independent studies). No differences were predicted by the model for net precipitation (80 %, Table 4, $P = 0.51$, two-sample Wilcoxon test) and runoff of YS and OG (Table 5, $P = 0.12$, two-sample Wilcoxon test). However, water loss through depth percolation was significantly lower in OG than in YS ($P < 0.001$, two-sample Wilcoxon test, Table 4). Evapotranspiration was higher in OG than YS, mainly due to higher transpiration in OG (Table 4, $P < 0.001$, two-sample Wilcoxon test). Soil moisture predicted by the model was significantly lower in OG than in YS (55 % and 63 %, respectively, $P < 0.001$, two-sample Wilcoxon test, Table 4).

3.2 Sensitivity to changes in climatic parameters

The model predicted changes both in the hydrological components and structure of the forests when simulations were run under different climatic scenarios (Figs. 6 and 7). We found similar soil moisture sensitivity of YS and OG to changes in rainfall parameters, with soil moisture decreasing to 32.5 % and 26.7 %, respectively (Fig. 6a, b). In both forests, decreases in $\eta < 80\%$ (mean depth of rainfall events) consistently produced that soil moisture decreased to $< 50\%$ (Fig. 6a, b). The influence of $1/\lambda$ (mean interval time between rainfall events) was negligible when η was kept constant in its current value (100 %, x-axis, Fig. 6a, b). The model consistently predicted less evapotranspiration (hereafter ETP) in comparison to current climate (Fig. 6c, d). In OG, ETP was reduced up to 94.4 mm yr^{-1} in the most extreme climatic scenario (upper left corner, Fig. 6d). In contrast, decreases in ETP in YS were < 50 mm yr^{-1} in the different climatic scenarios (Fig. 6c). Decreases of ETP in OG were consistently > 60 mm yr^{-1}, with changes in $\eta < 60\%$ and from increases in $1/\lambda > 120\%$ (Fig. 6d). Decreases in ETP of OG (e.g., > 35 mm yr^{-1}, for $\eta < 70\%$ Fig. 6d) were also detected when $1/\lambda$ was kept constant in 100 % (current value).

Structural variables of YS showed less sensitivity than OG to changes in climatic parameters (Fig. 7). We didn't detect distinct changes in basal area and above-ground biomass (AGB) in YS attributable to changes in climatic parameters (Fig. 7a, c). In contrast, in OG changes in rainfall parameters produced decreases in basal area up to 21 % (Fig. 7b, predicted total basal area of 62.6 m^2 ha^{-1}) and decreases of AGB up to 27 % (Fig. 7d, predicted AGB of 303.7 t C ha^{-1}). Main changes in basal area and AGB of OG occurred for reductions of $\eta < 70$ % and $1/\lambda$ higher than 130 % (Fig. 7b, d).

4 Discussion

4.1 Model performance

In this study, we developed and evaluated the performance of an individual- and process-based dynamic forest model that incorporates detailed calculations of water cycling in North Patagonian forests. The model allows the investigation of the dynamic linkage between rainfall tendencies and forest processes at local scales. Model results comparison (Figs. 4 and 5) with hydrological measurements from a young secondary stand were adequate considering that we compared simulations of 1 ha against measured samples from considerably smaller areas (400 m^2). Additionally, the model depicted well main forest hydrological components in comparison with hydrological balance in similar old-growth broad-leaved temperate rainforests in Chile and elsewhere (Table 4, independent studies). The model incorporates the state-of-the-art knowledge on hydrological controls on forest processes in temperate rainforests of southern Chile and was sensitive to changes in rainfall regimes (see also Sect. 4.2). Overall these results lend support to the performance of the developed model to predict the hydrological balance of temperate rainforests of southern South America.

Title Page

Abstract | Introduction

Conclusions | References

Tables | Figures

|◄ | ►|

◄ | ►

Back | Close

Full Screen / Esc

Printer-friendly Version

Interactive Discussion

4.2 Sensitivity to changes in rainfall regimes

A direct interpretation of changes in rainfall regimes is possible because the model account explicitly for changes in frequency and amount of rainfall events (Laio et al., 2001; Kumagai et al., 2004; Porporato et al., 2004). Amount of rainfall events alone can induce structural changes in the studied forest type (Fig. 7), but simultaneous changes in the frequency and amount of rainfall produced the strongest changes in the hydrology and structure of stands (Fig. 7). This result highlights the impact of the duration and frequency of periods of water stress on forest structure and growth.

Our results suggest that forests in the study region can be impacted by changes in rainfall regimes predicted for this century. In our study, rainfall scenario such as the one predicted for the study area (up to 50 % reduction in summer rainfall, business-as-usual scenario, DGF and CONAMA, 2006) can induce changes in both hydrological balance (up to 15 % decrease in ETP, Fig. 6) and structure of forests in this region (up to 27 % decrease in AGB, Fig. 7), even not considering the effects of global warming. Changes in rainfall regimes drove similar changes in soil moisture in forests varying in stand age (YS and OG, soil moisture decreasing to 32 %, Fig. 7). However, patterns of evapotranspiration (Fig. 6c, d), basal area and biomass contrasted strongly between stands (Fig. 7). The water-use efficiency concept implemented in the model to calculate transpiration (Eq. 8) implies that trees assimilating more biomass will demand a higher amount of water to grow. Accordingly, a higher water demand in OG than YS is predicted by the model due to a higher gross primary productivity of OG compared to YS (18.2 ± 1.2 compared to $31.6 \pm 2.3\,\mathrm{t\,C\,ha^{-1}\,yr}$, under current climate). We suggest that contrasting ETP and structural patterns between YS and OG under varied rainfall scenarios are mainly due to soil moisture limitations for biomass production in OG. These results also points to WUE as a sensitive parameter in our model to predict responses of forests under different climatic scenarios (see also Sect. 4.3).

4.3 Model limitations and research needs

In this study, we focused in developing an accurate model for depicting forest hydrology at local scales. It was beyond the scope of the present study to discuss model behavior along drought-to-moist gradients operating at regional scales. Expanding the range of applicability of the model for such analyses will certainly require an accurate and quantitative estimation of species-specific drought tolerance parameters (Bugmann and Cramer, 1998). Although tree species in southern South America can be order along drought gradients (Alberdi, 1995), such order has been experimentally tested for few tree species (Piper et al., 2007; Figueroa et al., 2010). After quantitatively deriving species-specific drought indices of tree species they can be easily incorporated into model calculations of the soil moisture threshold for the potential biomass production of trees (θ_{msw}, Eq. 13). Tree-rings can be also used to evaluate tree grow responses to past drought events (Orwig and Abrams, 1997) but first is necessary to disentangle the effects of competition, disturbance and other climatic effects (e.g., temperature) on tree grow. Recent studies have noticed that water-use efficiency varies inside the geographical distribution of a tree species (Figueroa et al., 2010) and among tree species (Piper et al., 2007) in SSA. Nevertheless, such variations have been experimentally tested in few study sites and for three out of the 11 tree species included in our study. Model formulation can be easily changed to incorporate physiological differences in the water use among tree species if required. In addition, water-use efficiency of forest stands may vary along forest succession and under drought conditions, but this has not been empirically proven in forests of SSA. Further experimental ecophysiological research is necessary to document water-use efficiency of tree species and along forest development in the study area in order to incorporate water-use efficiency as a species-specific parameter or a state (time dependent) variable in the model.

In this study, we deliberately excluded the influence of temperature on forest processes (e.g., tree growth) in order to isolate the impact of different rainfall regimes in model results. Temperature can modify individual tree growth by affecting

photosynthesis and respiration (Lambers et al., 1998), affect soil respiration (Ryan and Law, 2005), nutrients dynamics (Aerts and Chapin, 2000) and establishment of trees (Hobbie and Chapin, 1998). Another undergoing study analyzes the joined effect of temperature and rainfall regimes on forest processes in the study area (c.f. Gutiérrez,

5 2010). We deliberately excluded other processes (e.g., increased run off in slopes and soil moisture dynamics across multiple soil layers) mainly because of lowland and flat characteristics of the studied stands, and to keep simplicity in model formulations. Such processes should be included if the model is to be applied in forests located on slopes or in other soil conditions. In humid environments such as the study area where wet-

10 lands or saturated soils are prevalent, the water table is commonly present and may interact with ecological processes such as tree establishment and mortality (Díaz and Armesto, 2007; Díaz et al., 2007). Our model provides a convenient starting point to incorporate such an intertwined calculation of fluctuations in soil moisture and water table (Rodriguez-Iturbe et al., 2007) to explore its potential impacts on forest processes.

15   Differences in depth percolation predicted by the model compared to reported values (20 % less depth percolation, Table 4) can be explained by physical characteristics of soils on northern Chiloé Island. Depth percolation in the model is mainly depending on k_{soil} (i.e. soil texture dependent percolation rate at field capacity) that was calibrated specifically for soils of Chiloé. These soils, locally known as *ñadi* soils, have

20 high total pore volume, granular structure and high content of organic matter that affect the water-retention-curve, saturated hydraulic conductivity and infiltration properties (Janssen et al., 2004). Therefore, the application of our model in forests developing on soil types (e.g., soils originated from volcanic ashes, Andisols, Wright, 1965) will require a site-specific calibration of parameters k_{soil}, n, and z (Table 1). Differences in

25 forest composition may also explain differences in depth percolation results. For example, we compared model results with a forest with a mixed composition of broadleaved and caducifolius tree species (*Nothofagus obliqua*, Echeverría et al., 2007) that may differ in leaf area index and net precipitation throughout the year. Despite of differences associated with soil type characteristics and forest composition, the results presented

in Table 4 suggest that selected hydrologic parameters (e.g., α, f, and LAI_{max}, see Table 1) depicted well the canopy water retention capacity of temperate rainforests in SSA.

4.4 Model application

To our knowledge, this is the first application of a forest gap model in temperate rainforests of southern South America allowing dynamic calculations of the impacts of different rainfall regimes on forest processes. The developed model was built up over a previous forest gap model that incorporated main ecological processes driving forest dynamics in temperate rainforests of Chile (Rüger et al., 2007; Gutiérrez and Huth, 2012). The model developed here can help to elucidate the role that variations in rainfall play on forest ecological and hydrological processes. For example, the model can be used to explore the influence of seasonal droughts driven by El Niño Southern Oscillation (ENSO) and other climatic oscillations on forest process (e.g., Kumagai et al., 2009). ENSO-events have been found to amplify background tree mortality rates and cause extensive mortality of *Nothofagus* in SSA (Suarez et al., 2004) mirroring drought-induced mortality documented in other temperate rainforests (Allen et al., 2010). The model developed here is a convenient tool to assess the linkage between ENSO-driven drought events and their impact on forest processes in SSA.

To date, the implications of different logging strategies, changes in fire regimes, introduction of exotic tree species and forest fragmentation in the context of a changing climate remain poorly understood in SSA. These growing threats on the last remnants of primary forest in this region demand to understand the multiple dimensions of global change on forests functioning. The model presented here is particularly suitable for analyzing the impacts of multiple drivers of global change in this region because logging (Huth et al., 2004; Rüger et al., 2007) and fragmentation effects (Groeneveld et al., 2009; Putz et al., 2011) can be included in simulations of forest dynamics. The model is also a suitable tool to contribute in the development of management strategies to adapt forests to climate change (Millar et al., 2007).

Title Page

Abstract | Introduction

Conclusions | References

Tables | Figures

|◀ | ▶|

◀ | ▶

Back | Close

Full Screen / Esc

Printer-friendly Version

Interactive Discussion

Printer-friendly Version

Interactive Discussion

5 Conclusions

In this research we presented a forest gap model that allows the analysis of the impact of rainfall regimes on ecological and hydrological processes. The developed model was accurate for depicting forest hydrology at local scales (i.e. < 100 ha) and allows the analysis of the dynamical linkage of rainfall regimes, soil moisture, and individual tree growth. Using the model we demonstrated that forests in the study region can be impacted by changes in rainfall regimes predicted for this century. The developed model expands the range of applicability of gap models to assess climate change impacts in less study areas such as temperate forests of the Southern Hemisphere. The developed model is a step forward towards developing simple and general models to assess complex and dynamical processes operating at multiple spatial scales in forests.

References

Aerts, R. and Chapin, F. S.: The mineral nutrition of wild plants revisited: a re-evaluation of processes and patterns, Adv. Ecol. Res., 30, 1–67, 2000.

Alaback, P. B.: Comparative ecology of temperate rain-forests of the america along analogous climatic gradients, Rev. Chil. Hist. Nat., 64, 399–412, 1991.

Alberdi, M.: Ecofisiología de especies leñosas de los bosques higrófilos templados de Chile. Resistencia a la sequía y bajas temperaturas, in: Ecología de los Bosques Nativos de Chile,

edited by: Armesto, J., Villagrán, C., and Arroyo, M. K., Editorial Universitaria, Santiago, 279–300, 1995.

Allen, C. D., Macalady, A. K., Chenchouni, H., Bachelet, D., McDowell, N., Vennetier, M., Kitzberger, T., Rigling, A., Breshears, D. D., Hogg, E. H., Gonzalez, P., Fensham, R., Zhang, Z., Castro, J., Demidova, N., Lim, J. H., Allard, G., Running, S. W., Semerci, A., and Cobb, N: A global overview of drought and het-induced tree mortality reveals emerging climate change risks for forests, Forest Ecol. Manage., 259, 660–684, 2010.

Aravena, J. C., Carmona, M. R., Perez, C. A., and Armesto, J. J.: Changes in tree species richness, stand structure and soil properties in a successional chronosequence in Northern Chiloe Island, Chile, Rev. Chil. Hist. Nat., 75, 339–360, 2002.

Armesto, J. J., Rozzi, R., Smith-Ramírez, C., and Arroyo, M. T. K.: Conservation targets in South American temperate forests, Science, 282, 1271–1272, 1998.

Armesto, J. J., Smith-Ramírez, C., Carmona, M. R., Celis-Diez, J. L., Díaz, I., Gaxiola, A., Gutiérrez, A. G., Núñez-Avila, M., Pérez, C., and Rozzi, R.: Old-growth temperate rain forests of South America: conservation, plant-animal interactions, and baseline biogeochemical processes, in: Ecol Stud-Anal Synth, edited by: Wirth, C., Gleixner, G., and Heimann, M., Springer, New York, Berlin, Heidelberg, 367–390, 2009.

Asbjornsen, H., Goldsmith, G. R., Alvarado-Barrientos, M. S., Rebel, K., Van Osch, F. P., Rietkerk, M., Chen, J. Q., Gotsch, S., Tobon, C., Geissert, D. R., Gomez-Tagle, A., Vache, K., and Dawson, T. E.: Ecohydrological advances and applications in plant-water relations research: a review, J. Plant. Ecol.-UK, 4, 3–22, doi:10.1093/jpe/rtr005, 2011.

Barbour, M. M., Hunt, J. E., Walcroft, A. S., Rogers, G. N. D., McSeveny, T. M., and Whitehead, D.: Components of ecosystem evaporation in a temperate coniferous rainforest, with canopy transpiration scaled using sapwood density, New Phytol., 165, 549–558, 2005.

Bazzaz, F. A.: Physiological ecology of plant succession, Ann. Rev. Ecol. Syst., 10, 351–371, 1979.

Botkin, D. B.: Forest Dynamics: an Ecological Model, Oxford University Press, Oxford, 309 pp., 1993.

Brodribb, T. and Hill, R. S.: The photosynthetic drought physiology of a diverse group of Southern Hemisphere conifer species is correlated with minimum seasonal rainfall, Funct. Ecol., 12, 465–471, 1998.

Bugmann, H.: A review of forest gap models, Clim. Change, 51, 259–305, 2001.

Forest sensitivity to changes in rainfall regimes

A. G. Gutiérrez et al.

Title Page

Abstract	Introduction
Conclusions	References
Tables	Figures

◀ | ▶

◀ | ▶

Back | Close

Full Screen / Esc

Printer-friendly Version

Interactive Discussion

Bugmann, H. and Cramer, W.: Improving the behaviour of forest gap models along drought gradients, Forest Ecol. Manage., 103, 247–263, 1998.

Bugmann, H. K. M. and Solomon, A. M.: Explaining forest composition and biomass across multiple biogeographical regions, Ecol. Appl., 10, 95–114, 2000.

Christensen, J. H., Hewitson, B., Busuioc, A., Chen, A., Gao, X., Held, I., Jones, R., Kolli, R. K., Kwon, W.-T., Laprise, R., Magaña Rueda, V., Mearns, L., Menéndez, C. G., Räisänen, J., Rinke, A., Sarr, A., and Whetton, P.: Regional climate projection, in: Climate Change 2007: The Physical Science Basis. Contribution of Working Group I to the Fourth Assessment Report of the Intergovernmental Panel on Climate Change, edited by: Solomon, S., Qin, D., Manning, M., Chen, Z., Marquis, M., Averyt, K. B., Tignor, M., and Miller, H. L., Cambridge University Press, Cambridge, New York, 94 pp., 2007.

CIREN: Delimitación y Descripción de Microregiones para la Transferencia Tecnológica de IN-DAP, CORFO, Santiago, 99 pp., 1994.

Cunningham, S. C.: Photosynthetic responses to vapour pressure deficit in temperate and tropical evergreen rainforest trees of Australia, Oecologia, 142, 521–528, 2005.

di Castri, F. and Hajek, E.: Bioclimatología de Chile, Universidad Católica de Chile, Santiago, 1976.

Díaz, M. F. and Armesto, J. J.: Physical and biotic constraints on tree regeneration in secondary shrublands of Chiloe Island, Chile, Rev. Chil. Hist. Nat., 80, 13–26, 2007.

Díaz, M. F., Bigelow, S., and Armesto, J. J.: Alteration of the hydrologic cycle due to forest clearing and its consequences for rainforest succession, Forest Ecol. Manage., 244, 32–40, 2007.

Dingman, S. L.: Physical Hydrology, 2nd edn., Prentice Hall, New Jersey, 646 pp., 2002.

Donoso, P. J., Soto, D. P., and Bertin, R. A.: Size-density relationships in *Drimys winteri* secondary forests of the Chiloe Island, Chile: effects of physiography and species composition, Forest Ecol. Manage., 239, 120–127, 2007.

Echeverría, C., Newton, A. C., Lara, A., Benayas, J. M. R., and Coomes, D. A.: Impacts of forest fragmentation on species composition and forest structure in the temperate landscape of Southern Chile, Global Ecol. Biogeogr., 16, 426–439, 2007.

Figueroa, J. A., Cabrera, H. M., Queirolo, C., and Hinojosa, L. F.: Variability of water relations and photosynthesis in Eucryphia cordifolia Cav. (Cunoniaceae) over the range of its latitudinal and altitudinal distribution in Chile, Tree Physiol., 30, 574–585, doi:10.1093/treephys/tpq016, 2010.

Forest sensitivity to changes in rainfall regimes

A. G. Gutiérrez et al.

Title Page

Abstract	Introduction
Conclusions	References
Tables	Figures

Back | Close

Full Screen / Esc

Printer-friendly Version

Interactive Discussion

Gerten, D., Schaphoff, S., Haberlandt, U., Lucht, W., and Sitch, S.: Terrestrial vegetation and water balance – hydrological evaluation of a dynamic global vegetation model, J. Hydrol., 286, 249–270, 2004.

Groeneveld, J., Alves, L. F., Bernacci, L. C., Catharino, E. L. M., Knogge, C., Metzger, J. P., Putz, S., and Huth, A.: The impact of fragmentation and density regulation on forest succession in the Atlantic rain forest, Ecol. Model, 220, 2450–2459, doi:10.1016/j.ecolmodel.2009.06.015, 2009.

Gutiérrez, A. G.: Long-Term Dynamics and the Response of Temperate Rainforests of Chiloé Island (Chile) to Climate Change, Lehrstuhl für Waldwachstumskunde, Technische Universität München, Freising, Germany, 170 pp., 2010.

Gutiérrez, A. G. and Huth, A.: Successional stages of primary temperate rainforests of Chiloé Island, Chile, Perspect. Plant Ecol., doi:10.1016/j.ppees.2012.01.004, in press, 2012.

Gutiérrez, A. G., Armesto, J. J., and Aravena, J. C.: Disturbance and regeneration dynamics of an old-growth North Patagonian rain forest in Chiloe Island, Chile, J. Ecol., 92, 598–608, 2004.

Gutiérrez, A. G., Armesto, J. J., Aravena, J. C., Carmona, M., Carrasco, N. V., Christie, D. A., Peña, M. P., Pérez, C., and Huth, A.: Structural and environmental characterization of old-growth temperate rainforests of Northern Chiloe Island, Chile: Regional and global relevance, Forest Ecol. Manag., 258, 376–388, doi:10.1016/j.foreco.2009.03.011, 2009.

Hall, G. M. J. and Hollinger, D. Y.: Simulating New Zealand forest dynamics with a generalized temperate forest gap model, Ecol. Appl., 10, 115–130, 2000.

Haxeltine, A. and Prentice, I. C.: BIOME3: An equilibrium terrestrial biosphere model based on ecophysiological constraints, resource availability, and competition among plant functional types, Global Biogeochem. Cy., 10, 693–709, 1996.

Hobbie, S. E. and Chapin, F. S.: An experimental test of limits to tree establishment in Arctic tundra, J. Ecol., 86, 449–461, 1998.

Holdgate, M. W.: Vegetation and soils in the South Chilean Islands, J. Ecol., 49, 559–580, 1961.

Huber, A. and Iroume, A.: Variability of annual rainfall partitioning for different sites and forest covers in Chile, J. Hydrol., 248, 78–92, 2001.

Huth, A., and Ditzer, T.: Simulation of the growth of a lowland Dipterocarp rain forest with FORMIX3, Ecol. Model., 134, 1–25, 2000.

Title Page

Abstract | Introduction

Conclusions | References

Tables | Figures

|◄ | ►|

◄ | ►

Back | Close

Full Screen / Esc

Printer-friendly Version

Interactive Discussion

Huth, A. and Ditzer, T.: Long-term impacts of logging in a tropical rain forest – a simulation study, Forest Ecol. Manage., 142, 33–51, 2001.

Huth, A., Drechsler, M., and Kohler, P.: Multicriteria evaluation of simulated logging scenarios in a tropical rain forest, J. Environ. Manage., 71, 321–333, doi:10.1016/j.jenvman.2004.03.008, 2004.

Janssen, I., Kruemmelbein, J., Horn, R., and Ellies, A. S.: Physical and hydraulic properties of the ñadi soils in South Chile – comparison between untilled and tilled soil, Rev. Cienc. Suelo. Nutr., 4, 14–28, 2004.

Köhler, P.: Modelling anthropogenic impacts on the growth of tropical rain forests – using an individual-oriented forest growth model for the analyses of logging and fragmentation in three case studies, PhD Thesis, Center for Environmental Systems Research and Department of Physics, University of Kassel, Der Andere Verlag, Osnabrück, Germany, 2000.

Kumagai, T., Katul, G. G., Saitoh, T. M., Sato, Y., Manfroi, O. J., Morooka, T., Ichie, T., Kuraji, K., Suzuki, M., and Porporato, A.: Water cycling in a Bornean tropical rain forest under current and projected precipitation scenarios, Water Resour. Res., 40, W01104, doi:10.1029/2003WR002226, 2004.

Kumagai, T., Yoshifuji, N., Tanaka, N., Suzuki, M., and Kume, T.: Comparison of soil moisture dynamics between a tropical rain forest and a tropical seasonal forest in Southeast Asia: Impact of seasonal and year-to-year variations in rainfall, Water Resour. Res., 45, W04413, doi:10.1029/2008wr007307, 2009.

Laio, F., Porporato, A., Ridolfi, L., and Rodriguez-Iturbe, I.: Plants in water-controlled ecosystems: active role in hydrologic processes and response to water stress – II. Probabilistic soil moisture dynamics, Adv. Water Resour., 24, 707–723, 2001.

Lambers, H., Chapin, F. S., and Pons, T. L.: Plant Physiological Ecology, Springer, New York, 540 pp., 1998.

Lara, A., Little, C., Urrutia, R., McPhee, J., Alvarez-Garreton, C., Oyarzun, C., Soto, D., Donoso, P., Nahuelhual, L., Pino, M., and Arismendi, I.: Assessment of ecosystem services as an opportunity for the conservation and management of native forests in Chile, Forest Ecol. Manage., 258, 415–424, doi:10.1016/j.foreco.2009.01.004, 2009.

Little, C., Lara, A., McPhee, J., and Urrutia, R.: Revealing the impact of forest exotic plantations on water yield in large scale watersheds in South-Central Chile, J. Hydrol., 374, 162–170, doi:10.1016/j.jhydrol.2009.06.011, 2009.

Discussion Paper | Discussion Paper | Discussion Paper | Discussion Paper

Title Page

Abstract | Introduction

Conclusions | References

Tables | Figures

◄ | ►►

◄ | ►

Back | Close

Full Screen / Esc

Printer-friendly Version

Interactive Discussion

Luebert, F. and Pliscoff, P.: Sinopsis Bioclimática y Vegetacional de Chile, Editorial Universitaria, Santiago, 316 pp., 2006.

Lusk, C. H.: When is a gap not a gap? Light levels and leaf area index in bamboo-filled gaps in a Chilean rain forest, Gayana Bot., 58, 25–30, 2001.

Maidment, D. R.: Handbook of Hydrology, McGraw-Hill, USA, 1424 pp., 1993.

Millar, C. I., Stephenson, N. L., and Stephens, S. L.: Climate change and forests of the future: Managing in the face of uncertainty, Ecol. Appl., 17, 2145–2151, 2007.

Myers, N., Mittermeier, R. A., Fonseca, G. A. B. d., and Kent, J.: Biodiversity hotspots for conservation priorities, Nature, 403, 853–858, 2000.

Naulin, P.: Estimacion de la biomasa en un renoval de canelo (Drimys winteri J. R. et Foster) en la Comuna de Ancud., Facultad de Ciencias Forestales, Universidad de Chile, Santiago, 45 pp., 2002.

Navarro, C., Donoso, C., and Sandoval, V.: Los renovales de Canelo, in: Silvicultura de los bosques nativos de Chile, edited by: Donoso, C., and Lara, A., Editorial Universitaria, Santiago, Chile, 1999.

Neilson, R. P.: A model for predicting continental-scale vegetation distribution and water-balance, Ecol. Appl., 5, 362–385, 1995.

Orwig, D. A. and Abrams, M. D.: Variation in radial growth responses to drought among species, site, and canopy strata, Trees-Struct. Funct., 11, 474–484, 1997.

Oyarzun, C. E., Godoy, R., Staelens, J., Donoso, P. J., and Verhoest, N. E. C.: Seasonal and annual throughfall and stemflow in Andean temperate rainforests, Hydrol. Process., 25, 623–633, doi:10.1002/Hyp.7850, 2011.

Piper, F. I., Corcuera, L. J., Alberdi, M., and Lusk, C.: Differential photosynthetic and survival responses to soil drought in two evergreen Nothofagus species, Ann. For. Sci., 64, 447–452, 2007.

Porporato, A., Daly, E., and Rodriguez-Iturbe, I.: Soil water balance and ecosystem response to climate change, Am. Nat., 164, 625–632, 2004.

Prentice, I. C., Sykes, M. T., and Cramer, W.: A simulation-model for the transient effects of climate change on forest landscapes, Ecol. Model., 65, 51–70, 1993.

Putz, S., Groeneveld, J., Alves, L. F., Metzger, J. P., and Huth, A.: Fragmentation drives tropical forest fragments to early successional states: a modelling study for Brazilian Atlantic forests, Ecol. Model., 222, 1986–1997, doi:10.1016/j.ecolmodel.2011.03.038, 2011.

Forest sensitivity to changes in rainfall regimes

A. G. Gutiérrez et al.

Title Page

Abstract	Introduction
Conclusions	References
Tables	Figures

|◄ | ►|

◄ | ►

Back | Close

Full Screen / Esc

Printer-friendly Version

Interactive Discussion

R-Development-Core-Team: R: A Language and Environment for Statistical Computing., R Foundation for Statistical Computing, Vienna, Austria., 2005.

Rey, J. M.: Modelling potential evapotranspiration of potential vegetation, Ecol. Model., 123, 141–159, 1999.

Reynolds, J. F., Bugmann, H., and Pitelka, L. F.: How much physiology is needed in forest gap models for simulating long-term vegetation response to global change? Challenges, limitations, and potentials, Clim. Change, 51, 541–557, 2001.

Rodriguez-Iturbe, I., Porporato, A., Ridolfi, L., Isham, V., and Cox, D. R.: Probabilistic modelling of water balance at a point: the role of climate, soil and vegetation, P. Roy. Soc.-Math.-Phy., 455, 3789–3805, 1999.

Rüger, N., Gutiérrez, A. G., Kissling, W. D., Armesto, J. J., and Huth, A.: Ecological impacts of different harvesting scenarios for temperate evergreen rain forest in Southern Chile – a simulation experiment, Forest Ecol. Manage., 252, 52–66, doi:10.1016/j.foreco.2007.06.020, 2007.

Rutter, A. J. and Morton, A. J.: Predictive model of rainfall interception in forests, 3. Sensitivity of model to stand parameters and meteorological variables, J. Appl. Ecol., 14, 567–588, 1977.

Ryan, M. G. and Law, B. E.: Interpreting, measuring, and modeling soil respiration, Biogeochemistry, 73, 3–27, doi:10.1007/s10533-004-5167-7, 2005.

Shugart, H. H.: A Theory of Forest Dynamics. The Ecological Implications of Forest Succession Models, Springer, New York, 278 pp., 1984.

Sitch, S., Smith, B., Prentice, I. C., Arneth, A., Bondeau, A., Cramer, W., Kaplan, J. O., Levis, S., Lucht, W., Sykes, M. T., Thonicke, K., and Venevsky, S.: Evaluation of ecosystem dynamics, plant geography and terrestrial carbon cycling in the LPJ dynamic global vegetation model, Global Change Biol., 9, 161–185, 2003.

Smith, B., Prentice, I. C., and Sykes, M. T.: Representation of vegetation dynamics in the modelling of terrestrial ecosystems: comparing two contrasting approaches within European climate space, Global Ecol. Biogeogr., 10, 621–637, 2001.

Suarez, M. L., Ghermandi, L., and Kitzberger, T.: Factors predisposing episodic drought-induced tree mortality in Nothofagus – site, climatic sensitivity and growth trends, J. Ecol., 92, 954–966, 2004.

Trenberth, K. E., Jones, P. D., Ambenje, P., Bojariu, R., Easterling, D., Tank, A. K., Parker, D., Rahimzadeh, F., Renwick, J. A., Rusticucci, M., Soden, B., and Zhai, P.: Observations: Surface and Atmospheric Climate Change, in: Climate Change 2007: The Physical Science

Forest sensitivity to changes in rainfall regimes

A. G. Gutiérrez et al.

Title Page

Abstract	Introduction
Conclusions	References
Tables	Figures

◄◄ ►►

◄ ►

Back Close

Full Screen / Esc

Printer-friendly Version

Interactive Discussion

Basis. Contribution of Working Group I to the Fourth Assessment Report of the Intergovernmental Panel on Climate Change, edited by: Solomon, S., Qin, D., Manning, M., Chen, Z., Marquis, M., Averyt, K. B., Tignor, M., and Miller, H. L., Cambridge University Press, Cambridge, New York, 2007.

5   Veblen, T. T., Schlegel, F. M., and Oltremari, J. V.: Temperate broad-leaved evergreen forest of South America, in: Temperate Broad-Leaved Evergreen Forest, edited by: Ovington, J. D., Ecosystems of the World, Elsevier Science Publishers, Amsterdam, 5–31, 1983.

Venevsky, S. and Maksyutov, S.: SEVER: A modification of the LPJ global dynamic vegetation model for daily time step and parallel computation, Environ. Model. Softw., 22, 104–109,

10   2007.

Vose, J. V., J. M., Sun, G., Ford, C. R., Bredemeier, M., Otsuki, K., Wei, A., Zhang, Z. Q., and Zhang, L.: Forest ecohydrological research in the 21st century: what are the critical needs?, Ecohydrology, 4, 146–158, doi:10.1002/eco.193, 2011.

Wattenbach, M., Hattermann, F., Weng, R., Wechsung, F., Krysanova, V., and Badeck, F.:

15   A simplified approach to implement forest eco-hydrological properties in regional hydrological modelling, Ecol. Model., 187, 40–59, 2005.

Willson, M. F. and Armesto, J. J.: The natural history of Chiloé: on Darwin's trail, Rev. Chil. Hist. Nat., 69, 149–161, 1996.

Wright, C. A.: The volcanic ash soils of Chile, Report No. 2017, FAO, Roma, Italy, 201 pp.,

20   1965.

Zuñiga, R., Alberdi, M., Reyes-Díaz, M., Olivares, E., Hess, S., Bravo, L. A., and Corcuera, L. J.: Seasonal changes in the photosynthetic performance of two evergreen Nothofagus species in South Central Chile, Rev. Chil. Hist. Nat., 79, 489–504, 2006.

Title Page

Abstract | Introduction

Conclusions | References

Tables | Figures

|◄ | ►|

◄ | ►

Back | Close

Full Screen / Esc

Printer-friendly Version

Interactive Discussion

Table 1. Parameter descriptions and parameterization methods used for running simulations of North Patagonian rainforests located on Northern Chiloé Island, Chile. (a) literature, (b) calibrated with field data, (c) calculated, (d) calibrated using literature, (e) Meteorological data from EBSD.

	Description	Value	Units	Method	Reference
Climate					
$1/\lambda$	Mean interval time between rainfall events[**]	*	day^{-1}	e	This study
η	Mean depth of rainfall events[**]	*	$mm\,day^{-1}$	e	This study
T_μ	Mean daily temperature[**]	*	°C	e	This study
T_σ	Standard deviation daily temperature[**]	*	°C	e	This study
Rn_μ	Mean light intensity above canopy[**,***]	*	$\mu mol\,(photons)\,m^{-2}\,s^{-1}$	e	This study
Rn_σ	Standard deviation light intensity above canopy[**,***]	*	$\mu mol\,(photons)\,m^{-2}\,s^{-1}$	e	This study
Hydrologic Balance					
n	Vertically averaged porosity of the soil	0.757	–	a	1
z	Soil depth	52	cm	a	2
k_{soil}	Soil texture dependent percolation rate at field capacity	4	$mm\,day^{-1}$	a	3, 1
α	Slope of the canopy saturation curve	0.7	–	a, b	4
f	Parameter of the relationship LAI and canopy storage capacity	3	–	b	5
LAI_{max}	Maximum LAI of the studied forest	5.5	$m^2\,m^{-2}$	a	6
WUE	Water-use efficiency	9	$gCO_2\,kg^{-1}\,H_2O$	d	2
γ	Psychometer constant	65	$Pa\,K^{-1}$	a	7
L	Latent heat of vaporization of water	2.56×10^6	$J\,kg^{-1}$	d	7
Δ	Rate of change of saturated vapor pressure with temperature	c	$Pa\,K^{-1}$	c	7
θ_{wp}	Wilting point of the soil	0.125	%	a	8
θ_{fc}	Field capacity of the soil	0.3	%	a	8

* values indicated in Table 2; ** per season; *** calculated for dry ($P_d < 1\,mm$) and wet days ($P_d \geq 1\,mm$). References: (1) Jansen et al. (2004); (2) Díaz et al. (2007); (3) Sitch et al. (2003); (4) Wattenbach et al. (2005); (5) Rey (1999); (6) Lusk (2001); (7) Prentice et al. (1993), Haxeltine and Prentice (1996); (8) Maidment (1993).

Table 2. Parameter values used to run the weather generator under different climatic scenarios. *Current* represents climatic parameters used to run the model under current climatic conditions as described by instrumental records (meteorological station EBSD, time period 1998–2009). Radiation describes parameters Rn_μ and Rn_σ (the latter in brackets, $\mu\mathrm{mol\,(photons)\,m^{-2}\,s^{-1}}$). Temperature is mean daily temperature. *Scenarios* are the range of climatic parameters that were varied to run the model under different climatic scenarios (36 scenarios in total, see *Methods* for details). DJF: December to February (austral summer, growing season); MAM: March to May (austral autumn); JJA: June to August (austral winter), SON: September to November (growing season).

	Current climate		Scenarios	
Rainfall	$1/\lambda$ (1/days)	η (mm)	$1/\lambda$ (1/days)	η (mm)
DJF	0.90	8.3	0.99–1.36	4.2–7.5
MAM	0.55	12.8	0.55	12.8
JJA	0.29	16	0.29	16.0
SON	0.54	9.5	0.59–0.8	4.7–8.5
Temperature	T_μ (°C)	T_σ (°C)		
DJF	12.5	2.6		
MAM	10.1	3.6		
JJA	8.4	4.4		
SON	9.8	3.3		
Radiation	Rn_μ (Rn_σ) ($P_d < 1\,\mathrm{mm}$)	Rn_μ (Rn_σ) ($P_d \geq 1\,\mathrm{mm}$)		
DJF	1413.9 (317.0)	986.9 (378.2)		
MAM	701.2 (294.1)	398.8 (261.6)		
JJA	408.9 (159.1)	229.7 (139.4)		
SON	1065.5 (348.7)	640.8 (320.1)		

Table 3. Structure of the studied young-secondary forest (YS) compared to reported values for secondary stands (< 100 yr-old) dominated by *Drimys winteri* on Chiloé Island, Chile.

Species	This study		Literature*	
	Density (N ha^{-1})	Basal area (m^2 ha^{-1})	Density (N ha^{-1})	Basal area (m^2 ha^{-1})
Drimys winteri	1550	32.3	1800–4532	24.7–61.4
Eucryphia cordifolia	175	0.9	112–480	1.4–14.7
Myrtaceae[a]	1014	3.5	252–827	2.3–4.4
Nothofagus nitida	713	17.7	4–260	0.1–4
Podocarpaceae[b]	38	0.1	80–80	0.5–0.5
Weinmannia trichosperma	88	0.3	0–0	0–0
Others	287.5	1.9		
Total	3575	54.8	2431–7950	46–86.9

*Source: Navarro et al. (1999); Aravena et al. (2002); Naulin (2002); Donoso et al. (2007); Gutiérrez et al. (2009). Only detailed tree species present in YS. [a] *Tepualia stipularis, Myrceugenia* spp. and *Amomyrtus* spp.; [b] *Podocarpus nubigena, Saxegothaea conspicua.*

Table 4. Model estimates of the components of forest water balance in a young secondary forest (YS, 60 yr-old) and an old-growth forest (OG, > 500 yr-old) located on northern Chiloé Island, Chile. Model results are averaged results of 200 simulations per stand (see *Methods* for details). Literature are reported values of independent studies in Chilean temperate rainforests and comparable forests elsewhere. sd: standard deviation; %: percentage of annual rainfall; ETP: Evapotranspiration (sum of canopy interception and transpiration).

Variable	This study			Literature	
	mm yr^{-1}	sd	%	%	Source*
Young secondary stand (YS)					
Annual sum of rainfall	1999	±499			
Canopy Interception	381.5	±30.3	20.0	20–40	1
Depth percolation	980.7	±156.8	49.9	47	1
ETP	573.6	±35.1	30.3	45.2	1
Net precipitation	1617.2	±434.6	80.0	60–80	1
Runoff	722.9	±397.7	33.3		
Soil moisture		±12.5	62.5		
Transpiration	192.1	±18.8	10.3	22	1
Old-growth stand (OG)					
Annual sum of rainfall	1970	±381			
Canopy Interception	378.3	±33.6	19.9	17.8	2, 3
Depth percolation	907.4	±142.4	46.5	66.5	2
ETP	648.0	±44.1	34.3	19.9–33.3	2
Net precipitation	1591.8	±368.6	80.1		
Runoff	665.2	±321.9	31.8	30–55	4
Soil moisture		±13.3	55.3		
Transpiration	269.7	±26.1	14.4		
Potential evapotranspiration	769	±4		576–724	5

*(1) Broad-leaved evergreen forests, ca. 200 yr-old. Annual rainfall 2500 mm (Huber and Iroume, 2001; Oyarzun et al., 2011). (2) Mixed deciduous-broad-leaved old-growth forest. Annual rainfall 2400 mm (Echeverría et al., 2007). (3) Mixed broad-leaved and conifer forest, ca. 200 yr-old in New Zealand. Annual rainfall 3400 mm (Barbour et al., 2005). (4) Annual rainfall 1700–4500 mm, data from evergreen forests with 90 % cover (Lara et al., 2009). (5) Annual rainfall 2427–3991 mm (CIREN, 1994), meteorological stations of Castro and Punta Corona (Luebert and Pliscoff, 2006).

Title Page

Abstract | Introduction

Conclusions | References

Tables | Figures

|◄ | ►|

◄ | ►

Back | Close

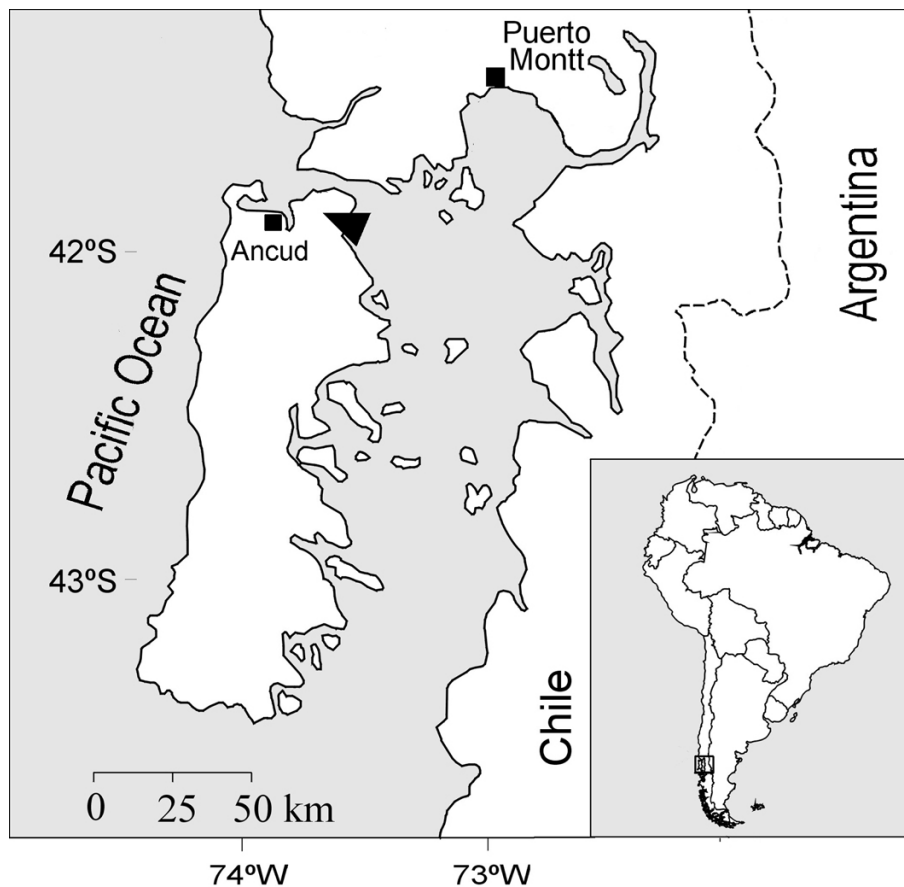Full Screen / Esc

Printer-friendly Version

Interactive Discussion

Fig. 1. Study site location (triangle) on Northern Chiloé Island, Chile.
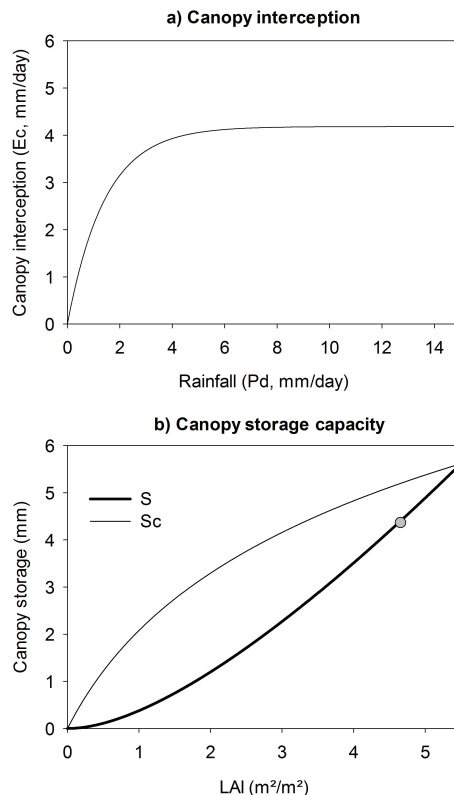
Fig. 2. Relationships used to calculate the canopy interception of a forest patch. **(a)** Canopy interception related to amount of rainfall events for a forest stand with LAI = 4.5. **(b)** Canopy storage related to LAI. *S* represents the canopy storage capacity and Sc the maximum storage capacity at a determined LAI. The thin line exemplifies the maximum canopy storage capacity attainable by a forest patch of 60 yr-old with LAI = 4.5. The grey dot shows the match between field data (Díaz et al., 2007) and model estimation of canopy storage capacity for a similar forest stand (LAI = 5).
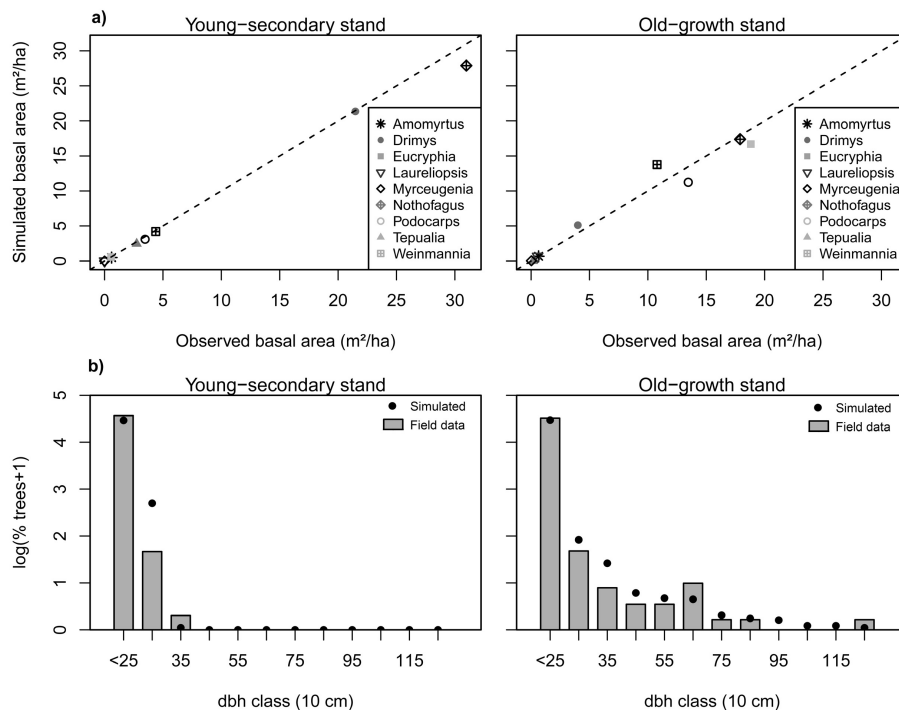
Fig. 3. Comparison of forest structure between observed (field data) and simulated species basal area **(a)** and dbh distribution **(b)** for both the young secondary (YS) and old-growth stand (OG) studied on Chiloé Island, Chile. Simulated old-growth structure obtained initializing the model with inventory data.
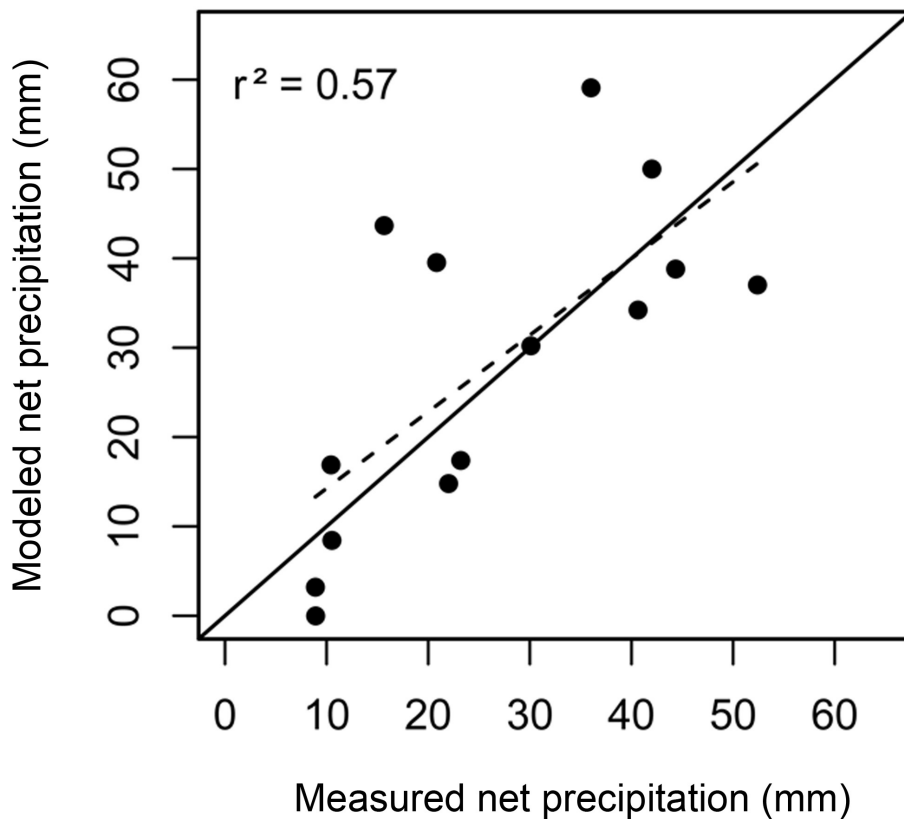
Fig. 4. Comparison between measured and modeled net precipitation. Dashed line represents a linear regression between measured and simulated values, the solid line represents the 1 : 1 relationship. All values are accumulated net precipitation for every measured rainfall event. Model results are for a forest patch of $400\,\text{m}^2$ with a LAI = 4.5.
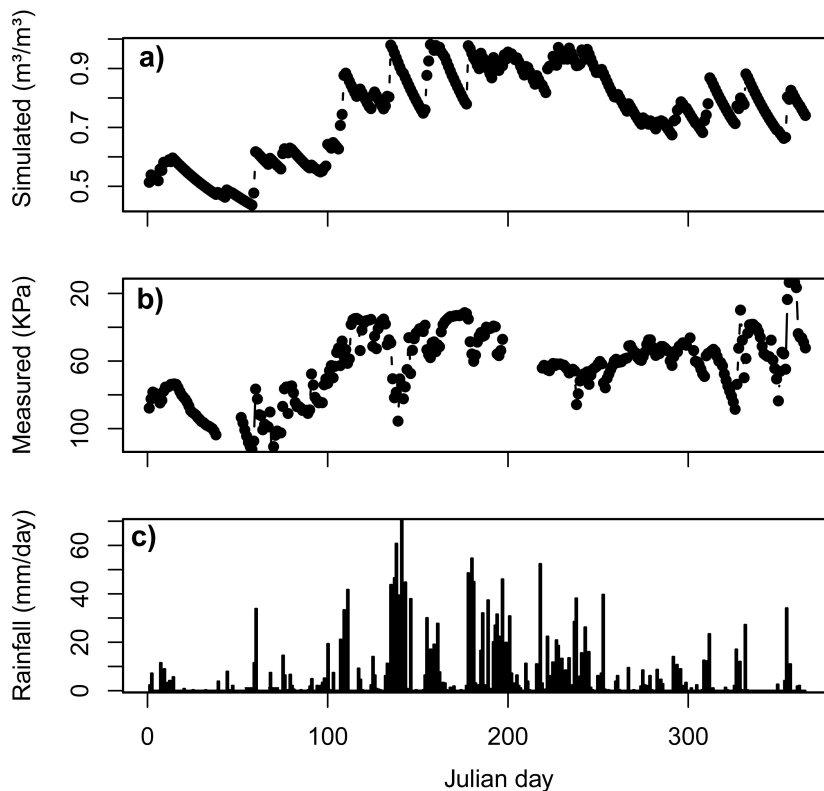
Fig. 5. Comparison between **(a)** simulated soil saturation and **(b)** measured soil matric potential during 2008. Data in **(a)** are simulation results for a forest patch of 400 m^2 with successional age of 60 yrs (LAI = 4.5). Data in **(b)** are daily mean values of three soil moisture sensors located randomly inside a plot of 400 m^2 (see also *Methods*). Soil parameters are the same as described in Table 2. Daily rainfall events during 2008 are shown in **(c)** for reference.
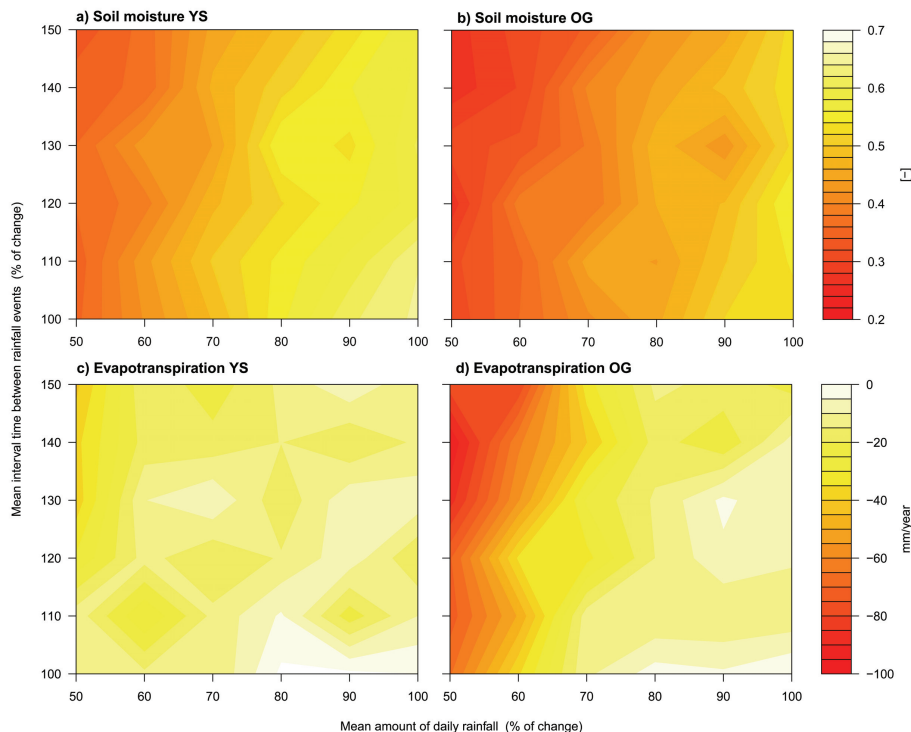
Fig. 6. Sensitivity of predicted soil moisture **(a, b)** and evapotranspiration **(c, d)** to changes in rainfall parameters. The y-axis represents the variation of mean interval of rainfall events ($1/\lambda$) from current climatic conditions (100 %) to 150 % increase of the current parameter value. The x-axis represents the variation in the mean amount of rainfall events (η) from current climatic conditions (100 %) to a 50 % decrease of the current parameter value. Results are the average of 30 simulations per scenario for a young-secondary (YS) and old-growth stand (OG). Results represent the difference between the average under current climatic conditions (see Table 2) and the average in every scenario.
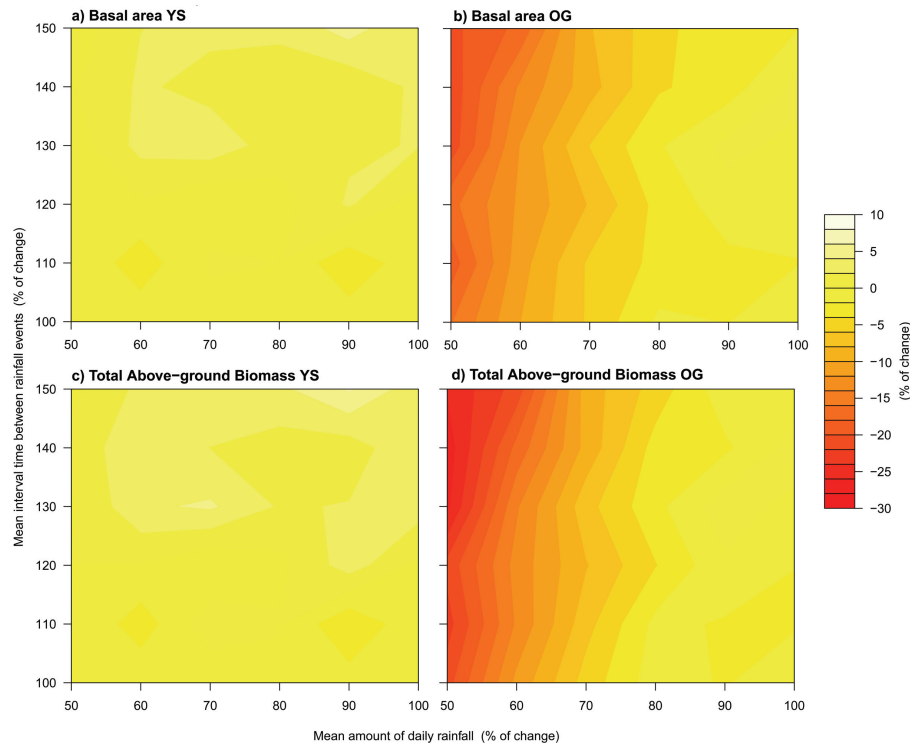
Title Page

Abstract | Introduction

Conclusions | References

Tables | Figures

|◄ | ►|

◄ | ►

Back | Close

Full Screen / Esc

Printer-friendly Version

Interactive Discussion

Fig. 7. Sensitivity of total basal area and above-ground biomass to changes in rainfall parameters. The y-axis represents the variation of mean interval of rainfall events $(1/\lambda)$ from current climatic conditions (100 %) to 150 % increase of the current parameter value. The x-axis represents the variation in the mean amount of rainfall events (η) from current climatic conditions (100 %) to a 50 % decrease of the current parameter value. Results are the average of 30 simulations for a young-secondary (YS) and old-growth stand (OG). Results represent the difference between the average under current climatic conditions (see Table 2) and the average in every scenario.

Title Page

Abstract | Introduction

Conclusions | References

Tables | Figures

◄◄ | ►►

◄ | ►

Back | Close

Full Screen / Esc

Printer-friendly Version

Interactive Discussion